

Development of Nanoparticle-Based Biodegradable Polymer Composite Film for Antifungal Drug Delivery in Prosthetic Joint Infection

Rupali Kale, Sanjeevani Shekhar Deshkar*, Pooja Dattatray Deshmane, Balasaheb Whagmare

Department of Pharmaceutics, Dr. D. Y. Patil Institute of Pharmaceutical Sciences and Research, Pimpri, Pune, Maharashtra, INDIA.

ABSTRACT

Background: Fluconazole is an antifungal agent of triazole class. Fluconazole is one of the most prescribed antifungal agents because of its excellent bioavailability, tolerability and side effect profile. To maintain drug concentrations within therapeutic levels in bone tissue for specific periods, antifungal agents must be re-administered when they are given systemically. **Aim:** The aim of the present study was to develop a nanoparticle-based implantable drug delivery system of antifungal drug fluconazole for Prosthetic Joint Infection and its *in vitro* and *in vivo* evaluation. **Materials and Methods:** Fluconazole loaded Chitosan Nanoparticles (CH-NP) were prepared by ionic gelation method and optimized for chitosan: TPP mass ratio, chitosan and fluconazole concentration. CH-NP were evaluated for particle size, polydispersity index, zeta potential, entrapment efficiency, FTIR, DSC, XRD and percent drug release. Nanoparticles were further incorporated in gelatine: chitosan composite film and formulations were optimized for chitosan: gelatin ratio, plasticizer concentration and cross-linker concentration. The developed composite film was tested for water absorption capacity, *in vitro* and *in vivo* biodegradation, toxicity and antifungal potency. **Results and Discussion:** The optimized CH-NP demonstrated 458 nm particle size, 82.39% entrapment efficiency and 77.4% drug release after 4 hr. The chitosan-gelatin ratio of 1:10, glycerine concentration of 5% and formaldehyde concentration of 0.01% resulted in desired *in vitro* properties and sustained drug release up to 10 hr. The developed formulation showed potent antifungal efficacy and *in vitro* biodegradation within 3 days. The *in vivo* biodegradation studies of films in rats showed complete degradation of implant within 7 days of implantation. Histopathology studies revealed no acute toxicity of implanted formulation. **Conclusion:** The developed Fluconazole loaded chitosan nanoparticle-based polymer composite film could be an effective formulation approach to prevent the fungal infections acquired during surgeries.

Keywords: Fluconazole, Nanoparticles, Chitosan, Implant, Prosthetic joint infection, Composite film

Correspondence:

Dr. Sanjeevani Shekhar Deshkar

Department of Pharmaceutics, Dr. D. Y. Patil Institute of Pharmaceutical Sciences and Research, Pimpri, Pune-411018, Maharashtra, INDIA.
Email: sanjeevani.deshkar@dypvp.eud.in, sanjeevanisd@yahoo.com

Received: 14-01-2024;

Revised: 27-02-2024;

Accepted: 13-04-2024.

INTRODUCTION

Joint replacement surgery involves removal of damaged joint and putting in a new one. Effective joint replacement surgery not only alleviates pain but also reinstates functionality and independence, ultimately enhancing the quality of life for patients. Although already a commonly undertaken procedure, the frequency of prosthesis implantation is anticipated to increase further. In India, more than 200,000 joint replacement surgeries were performed in 2020.¹ As by the next decade, majority of the Indian population will enter in their 50s' and 60s', the number of joint replacement

surgeries would steadily increase and be multi-fold compared to current status. While most joint arthroplasties offer painless functionality, a small percentage of patients may encounter device failure, necessitating additional surgery at some point in the lifespan of the implant.²

Prosthetic Joint replacement surgery associated Infection (PJI), although rare, is a major cause in failure of knee arthroplasty procedure. The majority prosthetic joint infections are bacterial and fungal infections are rare accounting for less than 1% of PJI cases. However, fungal infections are very difficult to treat and pose threat to patients' lives and burden to the health care industry. The main causative organism of most of the fungal infections is a member of the *Candida* species and prevalent in 80% of the PJI cases. In 15 to 20% of PJI cases, presence of fungal infections further leads to acquisition of other bacterial and mixed infections complicating the treatment.³



DOI: 10.5530/ijper.58.2s.50

Copyright Information :

Copyright Author (s) 2024 Distributed under Creative Commons CC-BY 4.0

Publishing Partner : EManuscript Tech. [www.emanuscript.in]

The major risk factors for fungal PJIs include, old age, diabetes mellitus, prior surgical procedures and bacterial infections, therapies of immunosuppressant, overexposure of antibiotics, antibiotic resistance, prolonged use of wound drainage etc.⁴ In most situations, Periprosthetic Joint Infection (PJI) must be managed with a comprehensive strategy that includes both surgical intervention and medication therapy. This could mean arthroscopic or open debridement without prosthesis removal, prosthesis resection without reimplantation, direct or one-stage arthroplasty exchange, which replaces the prosthesis immediately with a new one, or two-stage arthroplasty exchange, which replaces it gradually over time. Additional alternatives encompass arthrodesis, amputation, or the utilization of antimicrobial suppression without the necessity for surgical intervention.⁵

The adherence of bacteria and fungi to biomaterials, along with the formation of biofilms on foreign bodies, is generally acknowledged to play a vital role in the emergence of infections linked to implants.⁶ Microorganisms within a biofilm demonstrate a notable elevation in antibiotic resistance and are shielded from the immune system of the host. Managing bone infections poses a challenge, primarily because systemically administered antibiotics or antifungals face difficulties in effectively penetrating local bone tissues. Moreover, microorganisms adhere to orthopaedic implants and the bone matrix, either by forming a slimy film or by adopting an unusually slow metabolic rate, thereby avoiding the host's immune defences and antibiotics.⁷ In several instances, the implant can become the origin of infection and the sole existing recourse is to eliminate the implant and undergo a subsequent implantation.⁸ This procedure presents a distressing encounter for both the patient and the healthcare professional. Treating Periprosthetic Joint Infection (PJI) poses considerable challenges due to restricted blood circulation within the infected skeletal tissue. The condition is exacerbated by insufficient dispersion of antibiotics at the site of infection. Furthermore, managing the pathogen-associated biofilm is really challenging due to ineffective drug targeting. Increased systemic dose of antibiotic, in order to enhance tissue and biofilm penetration, is undesirable due to the risk of severe toxic side effects. Moreover, traditional therapy involving systemic antibiotics is costly, susceptible to complications, necessitates hospitalization and frequently proves ineffective. Nowadays, controlled release antimicrobial systems in the form of orthopaedic devices or implants are being employed as substitutes for conventional systemic treatments. Some of these alternative systems include PMMA bone cements infused with antibiotics, polymeric coatings with drug content and bioresorbable implants loaded with drugs, alongside the fracture fixation device. A prevalent approach for managing infections with orthopedic implants involves the use of antibiotics incorporated into clinical bone cements, typically composed of Polymethyl Methacrylate (PMMA). For almost four decades,

clinical trials have been conducted on several formulations of these non-biodegradable polymer cements to prevent or cure Pressure Injuries (PJI).⁹ Due to its non-biodegradable nature, PMMA necessitates additional surgical intervention for removal in instances of clinical failure, preventing the growth of new bone until its extraction. Furthermore, drawbacks include the limited bonding strength of PMMA to the implant surface and the documented occurrence of soft tissue encapsulation around PMMA.¹⁰ When PMMA bone cement releases antibiotic from the surface of implant, pores are formed on the surface and ultimately affect strength of the implant.¹⁰ Recent studies have shown that implantation of antifungal loaded biodegradable inserts during surgery can release the antifungal drug locally and prevent the acquisition of fungal infection or locally treat the acquired infection in the initial stages.¹¹

Fluconazole belongs to the triazole class and is classified as an antifungal agent. It can be administered orally, intravenously and topically. This triazole exhibits potent and specific activity against *Candida* species, making it a subject of extensive evaluation for the treatment of both localized and disseminated fungal infections. Fluconazole remains one of the most prescribed antifungal agents because of its excellent bioavailability, tolerability and fewer side effects.¹² To sustain therapeutic drug concentrations in bone tissue for specified durations, antifungal agents must be periodically reintroduced when administered systemically. Prolonged systemic delivery of antifungal agents may elevate the risk of systemic adverse effects or cause discomfort for the patient. Local sustained release of fluconazole from implants can reduce the side effects as compared to oral and intravenous administration.¹³ Several studies have demonstrated fluconazole efficacy in treating PJI locally.¹⁴ In view of this, the current study aims to design and develop Chitosan Nanoparticle (CH-NP) based biodegradable composite film for delivery of Fluconazole in order to promote its local delivery with sustained release and intended to be used for prophylaxis and treatment of prosthetic fungal joint infection. Fluconazole loaded nanoparticles were prepared by ionic gelation technique and process was optimized for drug entrapment.¹⁵ The developed NP were incorporated in gelatine and chitosan composite film and evaluated for drug content, drug release, acute toxicity and *in vivo* biodegradation.

MATERIALS AND METHODS

Materials

Fluconazole was supplied by Zim laboratories, Kalmeshwar, Nagpur, India. Low molecular weight Chitosan (CH) was purchased from Sigma-Aldrich, India. Gelatine, polyvinyl alcohol and Tripolyphosphate Sodium (TPP) were procured from Hi-Media, Mumbai. Organic solvents used for analysis were of analytical grade.

Methodology

Formulation of fluconazole loaded chitosan nanoparticles

The preparation of chitosan nanoparticles containing fluconazole was carried out through the ionic gelation method, utilizing sodium Tripolyphosphate (TPP) as the crosslinking agent. The formulation was optimized for Chitosan to TPP mass ratio and fluconazole concentration by using following procedure.

Identification of nanoparticle region

Low Molecular Weight (LMW) CH was dissolved in aqueous solution of 1% acetic acid to form different concentration (2, 3 mg/mL) of CH solution. The chitosan solution was kept overnight at room temperature and the pH of the resultant solution was determined. Subsequently, it underwent filtration using a syringe filter to eliminate any remaining insoluble particles.¹³ A solution of TPP was prepared by dissolving it in distilled water at a concentration of 1, 2 and 3 mg/mL. This TPP solution was gradually added dropwise to the chitosan solution under continuous magnetic stirring. Various changes in visual appearance of solution during titration with TPP solution was observed; viz. solution, aggregates and opalescent suspension and precipitation. The region of an opalescent suspension was identified as nanoparticle region (Table 1).

Optimization of CH: TPP mass ratio

Chitosan (2 mg/mL) was dissolved in aqueous acetic acid (1%v/v) solution. To 10 mL of this solution, 30 mg of Fluconazole (FZ) was added and dissolved. TPP at the concentration of 2 mg/mL was added drop wise to 10 mL of fluconazole containing chitosan solution through micropipette under magnetic stirring at room temperature.¹⁴ The volume of TPP solution was varied according to the ratio of CH:TPP (4:1, 3.5:1, 3:1, 2.5:1) to obtain nanoparticle dispersion. The resulting formulations (P1 to P4) were evaluated for percent entrapment and percent transmittance (Table 2).

Optimization of CH and FZ concentration in CH-NP

FZ loaded chitosan nanoparticles (FZ CH-NP) were prepared at different concentration levels of chitosan (2 and 3 mg/mL) and fluconazole concentration (1, 2 and 3 mg/mL) using method mentioned above at CH:TPP mass ratio of 2.5:1. Each formulation was prepared in triplicate (Table 3) and evaluated for FZ entrapment efficiency and percent drug release.¹⁶

Lyophilisation of optimized nanoparticle formulation

In order to conduct the solid-state characterisation, FZCH-NP was separated from suspension by centrifugation at 16000 rpm at 14°C for 30 min. The supernatant was removed and nanoparticle pellet was obtained by lyophilisation process (Martin Christ, Alpha 1-2 LD plus, Germany). Lyophilized samples were further evaluated for FTIR, DSC and XRD.

Evaluation of fluconazole loaded chitosan nanoparticles (FZ CH-NP)

Percent transmittance measurement

To assess the relative transmittance of the nanodispersions, optical transmittance was gauged at 600 nm within the visible range.¹⁷ This measurement was conducted using a double-beam UV spectrophotometer (Shimadzu, 1800, Japan).

Particle size analysis and zeta potential

Deionized water was used to dilute the optimised chitosan nanoparticle dispersion (1 to 5 mL). At a scattering angle of 90°, photon correlation spectroscopy (Malvern, Nano Series ZS, UK) was used to evaluate the particle size distribution of the resultant sample.¹⁸ The dispersion of chitosan nanoparticles was measured for its average diameter (X_{90}) and polydispersity index. Additionally, the Zeta potential was measured using a Zetasizer after diluting samples with a conducting solution (Malvern, Nano Series ZS, UK).

FZ Entrapment efficiency

The percentage of FZ entrapment in CH-NP was determined using a dialysis membrane. This method enables separation of free drug from the NP by dialysis. The dialysis membrane (Himedia, MW cutoff 10Kda) was soaked overnight in a medium to ensure complete wetting. A 5 mL dispersion of FZ CH-NP was introduced into the membrane bag and the ends were securely tied. The bag was then immersed in 100 mL of mixture of methanol: distilled water (1:4) and stirred at 100 rpm using a magnetic stirrer. The spectrophotometric analysis of untrapped FZ was performed at 261 nm by withdrawing 5 mL sample.¹⁹ The FZ entrapment was calculated as follows.

$$\% \text{ Entrapment efficiency} = \frac{(\text{total amount of drug} - \text{free amount of drug})}{(\text{total amount of drug})} \times 100$$

In vitro drug release study

Drug release studies for fluconazole-loaded nanoparticles were conducted using a dialysis bag method (MW cutoff of 11KDa) in a modified dissolution apparatus USP Type I (Veego, DT60, India). Briefly, The pre-soaked membrane bag was filled with a volume of 5 mL of the aqueous CH-NP dispersion and the ends were secured to the dissolving assembly's basket rod.²⁰ The bag was inserted into 100 mL of phosphate buffer of pH 7.4 as dissolution medium at 37±0.50°C with 100 rpm stirring speed for 6 hr.¹⁰ At intervals of 15 min, 5 mL aliquots were taken out, filtered using disposable Nylon syringe filter (0.22 µm) and the fluconazole content was measured at 261 nm with a UV spectrophotometer.²¹ To compensate for any loss during sampling, an equivalent volume of 5 mL of fresh dissolution medium was added. The results of the drug release study were reported as mean of three observations.

Characterization of Lyophilized Chitosan Nanoparticle (CH-NP)

Fourier Transform Infrared analysis (FTIR)

The presence of fluconazole in CH-NP was verified using FT-IR analysis (Shimadzu, 8400S, Japan). The physical mixture of samples and potassium bromide were mixed and placed in sample holder to capture the FT-IR absorption spectra.^{22,23}

Differential Scanning Calorimetry

Differential Scanning Calorimetry (DSC) was employed to verify the physical state of Fluconazole (FZ) within the Chitosan Nanoparticle (CH-NP) formulation using equipment from Mettler Toledo (DSC 3, Switzerland). The temperature range of 30-400°C was applied to heat each sample (2-4 mg) in crimped aluminium pans at a scanning rate of 10°C/min under a nitrogen atmosphere.²⁴

X-ray Diffraction Studies

X-ray diffraction analysis was conducted using Cu K α rays. The voltage of 40 kV was used and a current of 25 mA was utilized on the Bruker D 8 Advanced instrument from the USA. The samples were scanned from 10 to 60° at 2 θ position. Diffraction patterns for FZ, its physical mixture with polymer and CH-NP formulation were acquired during the experiment.²⁵

Formulation of CH-NP loaded composite film

The chitosan solution (1% w/v) in acetic acid (100 mL of 1% v/v) was prepared and left to stand overnight at room temperature. Gelatine solution (10% w/v) was prepared by solubilizing gelatine in 100 mL distilled water at 70°C with continuous stirring. Chitosan and gelatine solutions were blended with stirring at various ratios (1:10, 1:20, 1:30 and 1:40). Prepared fluconazole nanoparticles were dispersed in gelatine-chitosan solution followed by addition of glycerine, as a plasticizer, at different concentrations (1, 2.5, 5 and 10%) under continuous overhead stirring. To study the effect of crosslinking on composite film, various concentrations of formaldehyde were also added to the above solution. The resulting solution was poured into petri plates and dried at 30°C under vacuum. The formulations (Tables 4, 5 and 6) were assessed for thickness, folding endurance and percentage water absorption to optimize the gelatine to chitosan ratio, the concentration of the plasticizer (glycerine) and concentration of formaldehyde.²⁶⁻²⁸

Evaluation of CH-NP loaded composite film

Initially prepared implants were evaluated for the physical properties such as, thickness and folding endurance for selection of the ratio of the gelatin and chitosan and optimization of concentration of plasticiser.

Thickness

The thickness of prepared gelatin-chitosan films was measured using Vernier Calliper (Mitutoyo corp, Japan) at four different sides and centre of the film and the average was assessed.²⁹

Folding endurance

The folding endurance of the prepared film was evaluated by repetitively folding one film at a time until it reached the point of breakage. The folding endurance value was calculated by determining the number of consecutive folds the film could endure at the same location without breaking.³⁰

Percent water absorption capacity

A Preweighed film (1x1 cm) was immersed in 15 mL of distilled water and the film's weight was recorded at intervals of 1, 2, 3 and 24 hr. The water absorption capacity of the film was assessed in triplicate and computed using the formula provided below.³¹

$$\text{Water absorption capacity (\%)} = \frac{(\text{final weight} - \text{initial weight})}{\text{initial weight}} \times 100$$

In vitro biodegradation

In vitro biodegradation study of crosslinked films at 0.01, 0.02 and 0.03% concentration of crosslinking agent using lower (1:10) and higher (1:40) ratios of chitosan: gelatin was carried out. The film (50 mg) was weighed to approximately and then immersed in 100 mL of 1% pepsin solution at 37°C with occasional shaking to determine its biodegradation. The films were checked periodically for changes after every 2 hr till complete degradation.³²

Content uniformity

The content of each film formulation was measured at the four corners and centre. Five samples of film formulation were measured. Each piece was dissolved in methanol and filtered through syringe filter. After appropriate dilutions the aliquots were examined by High-Performance Liquid Chromatography (HPLC) was conducted using a quaternary gradient system, Lachrom 2000, which included an L-7100 Merck Hitachi pump, UV-visible detector (L-7400) and a Kromasil C18 column (250mmx4.6mm, 5 μ m). The HPLC mobile phase comprised acetonitrile: phosphate buffer at pH 4 (60:40), with UV detection set at 261 nm and a column temperature of 37°C. The flow rate for HPLC was adjusted to 1 mL/min, with an injection volume of 20 μ L. The entire analysis was completed within 8 min.^{33,34}

In vitro drug release

Films were immersed in 40 mL phosphate buffer pH 7.4 at 37°C for 3 days in semi-static conditions, to determine the kinetics of fluconazole release from the films. 1 mL samples were collected and filtered by syringe filter (0.22 μ m) at time intervals, 0, 0.5, 1, 2, 4, 6, 8 and 10 hr. The sample removed was replaced with fresh phosphate buffer pH 7.4. The release of FZ at each time interval

was assessed with HPLC using conditions mentioned in previous section.³⁵

Antifungal activity of Film

Culture of *C. albicans* was grown for 24 hr on Sabouraud dextrose agar plate at 37°C in anaerobic condition. The fungal strains were collected and resuspended in 10 mL nutrient broth and adjusted to 1×10^8 CFU/mL by observing turbidity against McFarland solution. Antifungal activity of FZ CH-NP loaded film was compared with equivalent quantity of pure drug and placebo film. Preweighed samples of pure drug, prepared antifungal film (equivalent to drug quantity) or placebo films were suspended in nutrient broth containing 1×10^8 CFU/mL culture of *C. albicans*. Antifungal activity of samples was determined by withdrawing sample of 1 mL from at 0, 2, 4 and 6 hr of contact time from above solutions respectively and dispersed in pre-sterilized Sabouraud dextrose agar media at 40°C. The media was poured into the petri dish and incubated at 37°C for 48 hr in an anaerobic chamber. After incubation, the plates were removed from incubator and the colonies were counted by using colony counter. *C. albicans* grown on the sabouraud dextrose agar plate served as control. Growth inhibition of *C. albicans* was determined by comparing sample colony count with control count.³³⁻³⁶

In vivo biodegradation study

Male Wistar rats, with weights ranging from 180 to 250 g, were chosen and accommodated in five groups, each consisting of six animals, under standard laboratory conditions, including controlled temperature and a light/dark cycle. The rats were provided with free access to standard pellet food and water. Prior to the experiment, the animals underwent a minimum acclimatization period of 10 days in the laboratory environment.³⁷ The treatment and care of the animals in this study adhered to the guidelines recommended by the CPCSEA committee for the control and supervision of experiments on animals. Approval for the experimental protocol was obtained from the institutional animal ethical committee. Group 1 served as the control group with no treatment, Group 2 received a placebo film and Groups 3 and 4 were administered FZ film and FZ CH-NP loaded film, respectively.³⁸

The animals were anaesthetized by administering Intra Peritoneal (IP) injection of ketamine (30 mg/kg) and xylazine (12 mg/mL). The implantation site of each animal was shaved by using the blade. The operating site were disinfected by using Isopropyl Alcohol (IPA) 70% in distilled water and allowed it to dry for 30 sec. Deep skin incision (10-12 mm) in thigh region and exposing bone was done at the site using the sterile surgical blade no. 22. Pouch was formed on both sides of the incision and an implant was placed in each pocket. Following implantation, the incision was closed using non-absorbable surgical black-braided silk thread. Surgical site was again disinfected using 70% IPA and dressing was done after application of Betadine as antiseptic.³⁹

Each animal was given dose of Diclofenac injection (2mg/kg) as analgesic and ceftriaxone (2mg/kg) as antibiotic after every 4 days till completion study. Biodegradation of implant was observed visually by removing suture and scarifying one animals of group 3, 4 and 5 by operating implant site after 2, 5, 7, 14, 21 days respectively after implantation. Histopathology was performed after 22 days to observe inflammation after implantation.⁴⁰

Histopathology Studies

After the period of the 21-day, rats from every group suffered euthanasia through carbon dioxide suffocation and an overdose of thiopental sodium (75 mg/kg). Subsequently, the implant was extracted along with the surrounding tissues. Tissues adjacent to the implant were preserved in a 10% formalin solution. Subsequently, the tissue samples underwent dehydration in an automatic tissue processor, progressing through a series of gradually increasing alcohol percentages before being embedded in paraffin wax. Using an embedding machine, the tissue samples were microtomed and stained with dyes, hematoxylin and eosin. In order to look for any signs of inflammation near the implant, the resultant samples were examined under a light microscope.

RESULTS AND DISCUSSION

Identification of nanoparticle region

The chitosan nanoparticles were prepared by ionic gelation technique. Chitosan is a weakly basic polymer with pKa 6.3. Below this pH, it appears in protonated form ($R-NH_3^+$). The positively charged chitosan ions are crosslinked by polyvalent anions like Tripolyphosphate to form small nanoparticles by ionic gelation. The degree of crosslinking and formation of NP depends on various factors including, chitosan concentration, Sodium Tripolyphosphate (TPP) concentration, CH:TPP mass ratio, volume of TPP added to chitosan solution etc. In order to identify the nanoparticle region, varying concentration of TPP solution (1, 2 and 3 mg/mL) was slowly added to two different concentrations of chitosan solutions (2 and 3mg/mL) and phase transition was observed. During this titration, three kinds of the phenomena were observed; clear solution, opalescent suspension and precipitation. Opalescent region was identified as nanoparticle region. The volume of TPP required to be added in chitosan solution to obtain opalescent region was determined for different concentration of chitosan and the range was noted (Table 1). It was observed that TPP volume required for nanoparticle was increased when chitosan concentration was increased whereas increase in TPP concentration decreased the volume requirement of TPP for nanoparticle formulation. At lower volume of TPP added to chitosan solution, very light colour was developed which indicated starting point of nanoparticle formation. As more amount of TPP was added, the ionic gelation process resulted in formation of nanoparticle indicated by opalescent region. Further addition of TPP volume, leads to aggregation of CH-NP due to reduction in surface charge

Table 1: Volume range of Sodium Tripolyphosphate (TPP) for nanoparticle region.

Code	Chitosan (mg/mL)	TPP (mg/mL)	TPP Volume range (mL)		
			Clear	Opalescence	Aggregation
C1	2	1	Till 4.6	5.4 to 6.4	6.4 above
C2	2	2	Till 2.8	3.1 to 4.2	4.2 above
C3	2	3	Till 1.2	1.4 to 2.6	3.0 above
C4	3	1	Till 4.5	5.6 to 7.2	8.8 above
C5	3	2	Till 2.8	4.4 to 5.8	7.2 above
C6	3	3	Till 1.9	2.9 to 4.1	4.5 above

Table 2: Optimization of CH:TPP mass ratio.

Formulation	Chitosan: TPP mass ratio	Percent transmittance (%)	Percent entrapment (%)
P1	2.5:1	76.3±0.3	55.6±1.5
P2	3:1	83.5±0.2	52.4±1.5
P3	3.5:1	86.1±0.8	45.0±1.1
P4	4:1	89.6±0.6	33.4±1.4

Mean ±SD (n=3).

Table 3: Optimization of chitosan and fluconazole concentration.

Code	X1	X2	Percent transmittance (%)	Percent entrapment (%)	% Drug Release after 4 hr
	Chitosan (mg/mL)	Fluconazole (mg/mL)			
B1	2	1	62.4±0.9	70.1±1.1	84.3±2.1
B2	2	2	78.4±0.6	80.3±1.2	77.0±1.9
B3	2	3	51.9±0.7	60.7±1.1	81.2±1.6
B4	3	1	61.4±0.8	60.9±1.1	85.7±1.4
B5	3	2	76.5±1.2	70.8±1.1	86.1±1.7
B6	3	3	79.7±1.5	59.1±1.2	83.1±1.9

Mean±SD (n=3).

as indicated by precipitation region. Thus, considering opalescent region as nanoparticle region, the volume of TPP to obtain this region was considered to be optimum. For further study, chitosan concentration was optimized to be 2 mg/mL and TPP was also fixed at 2 mg/mL.

Optimization of CH: TPP mass ratio

For selection of appropriate CH: TPP mass ratio, different formulation with varying CH:TPP ratios were prepared and evaluated for percent transmittance and percent entrapment (Table 2). The other formulation parameters viz., chitosan concentration, fluconazole concentration, stirring speed and temperature were kept constant.

The high degree of deacetylation and protonation is responsible for greater positive charge and large number of potential cross-linking sites on chitosan molecules. Addition of TPP causes neutralization of protonated amino group leading to

cross-linking of chitosan nanoparticle. At higher CH:TPP mass ratio (4:1) due to the lower amount of TPP used inadequate cross linking could have occurred hence opalescent colour was not observed. The entrapment efficiency was found to be lower (33.4±1.4 and 45±1.1 for P4 and P3 respectively). Formulation with CH:TPP mass ratio 2.5:1 was selected for further study as stable opalescent region was observed for this ratio with highest entrapment efficiency (55.6 ±1.4%).

Optimization of CH and FZ concentration in CH-NP

In order to study the effect of chitosan concentration and fluconazole concentration on drug entrapment in CH-NP, different formulations of fluconazole chitosan nanoparticle were prepared as shown in Table 3. It was observed that as concentration of chitosan was increased, fluconazole entrapment was decreased. Highest entrapment was obtained at chitosan concentration 2 mg/mL. This could be due to higher viscosity of chitosan at

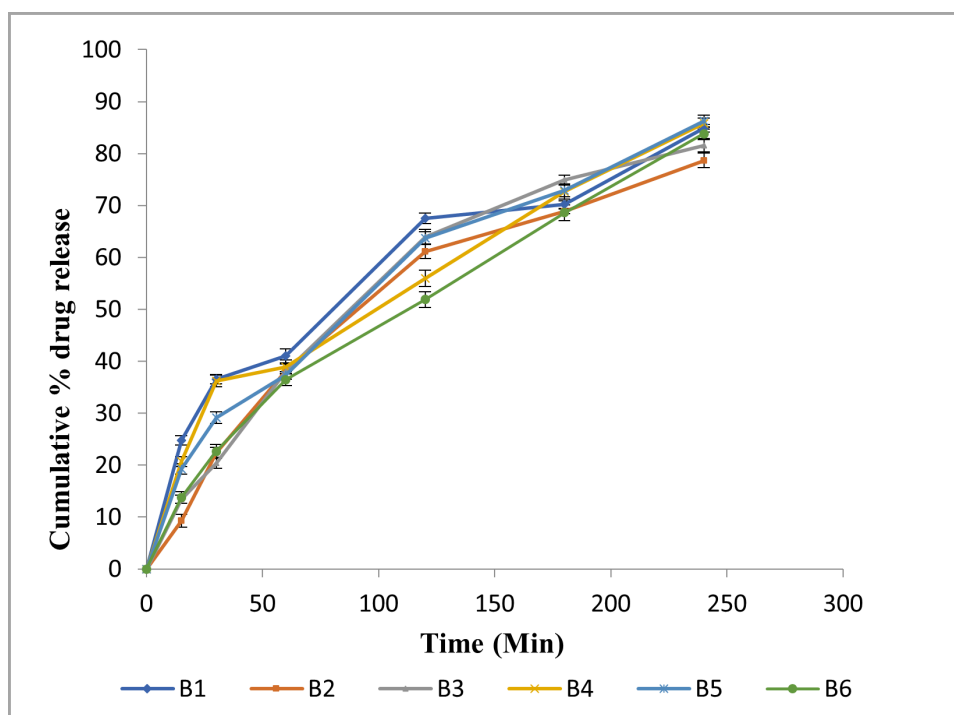


Figure 1: Cumulative percent drug release from NP formulation.

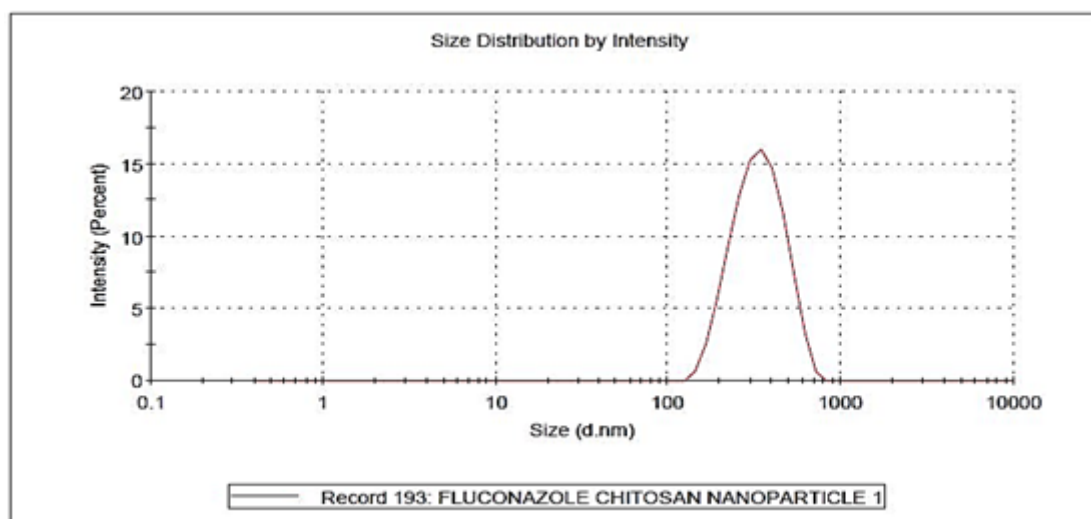


Figure 2: Particle size analysis graph of fluconazole CH-NP.

higher concentration resulting in lower drug entrapment. Higher amount of precipitation was observed at 3 mg/mL of chitosan concentration. Hence, 2 mg/mL of chitosan concentration was found to be suitable.

FZ concentration also found to affect the entrapment efficiency in CH-NP. Increase in FZ concentration from 1 to 2 mg/mL, increased its entrapment in NP whereas further increase in FZ concentration to 3 mg/mL, decreased the FZ entrapment.

Effect of these variables on drug release from CH-NP was also studied and the results are depicted in Figure 1. FZ release from CH-NP formulations B1 to B6 was found to be in the range of

77.0% to 86.1% after 4 hr of dissolution study. The drug release profile exhibited a biphasic pattern, characterized by an initial burst release followed by a sustained release of the drug. The drug release data was analysed using models such as Korsmeyer-Peppas, Higuchi matrix model, first-order and zero-order to elucidate the underlying rate and mechanism of drug release. Additionally, the correlation coefficient was obtained from time and cumulative drug release graph to determine the best-fit kinetics. The outcome of the model with correlation coefficient values suggested Fickian diffusion (K-P model n value=0.5) as the predominant drug release mechanism, except for formulations B2 and B3, which

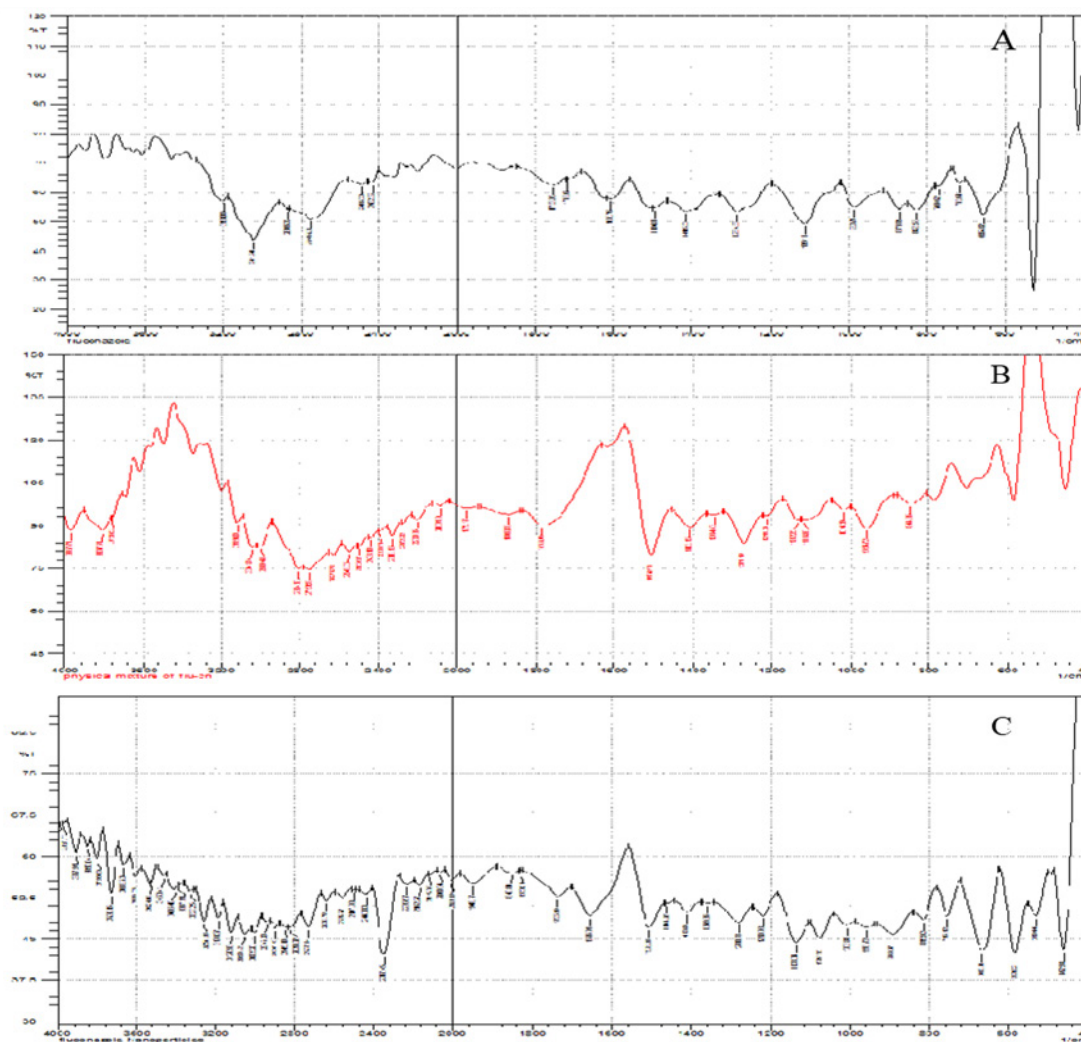


Figure 3: FT-IR spectrum of A) fluconazole, B) Physical mixture and c) fluconazole loaded chitosan nanoparticle.

exhibited a non-fickian drug release mechanism (K-P n value between 0.5 to 0.9). Based on the result of encapsulation efficiency and considering the requirement of high drug loading in final formulation, formulations B2, with 2 mg/mL drug concentration and 2 mg/mL chitosan concentration, was selected for further investigation as an optimized formulation. The particle size (X_{50}) of optimized B2 formulation was found to be 458.5 nm (Figure 2). Slightly higher size of chitosan nanoparticle could be due to neutralisation of chitosan by TPP to form larger size of nanoparticle. This was consistent with the polydispersity index of chitosan nanoparticle which was 0.58 that shows wide particle size distribution. In case of zeta potential analysis, positive zeta potential value (+0.98) was detected; lower zeta potential results could be due to neutralization of protonated chitosan.

Characterization of lyophilized fluconazole loaded chitosan nanoparticle

FTIR

FTIR investigations were carried out to evaluate the interaction between CH-TPP and CH-FZ within FZ CH-NP (Figure 3). The FT-IR of fluconazole indicated characteristic peaks at 3198 cm⁻¹ representing protonated amino group, a broader peak at 3300-2400 cm⁻¹ representing OH group, 3041.84 representing aromatic C-H stretching, 1415 cm⁻¹ C=C stretching, 1494 cm⁻¹ C=N and 1284 cm⁻¹ representing C-F. FTIR of physical mixture indicated all the characteristic peaks of fluconazole. The characteristic peak of chitosan was observed at 3198 cm⁻¹ representing protonated with a peak at the amino group 1114.89 cm⁻¹ representing C-O-C. In FTIR spectra of CHNP, the peak of protonated amino group was observed at 3190.37 cm⁻¹. Presence of P=O group at 1132.25 cm⁻¹ indicated interaction of TPP and CH in CHNP. As the major peaks of fluconazole were intact, no interaction was observed in chitosan and fluconazole. There is possibility of weak interaction in chitosan and fluconazole by hydrogen bonding as the peak

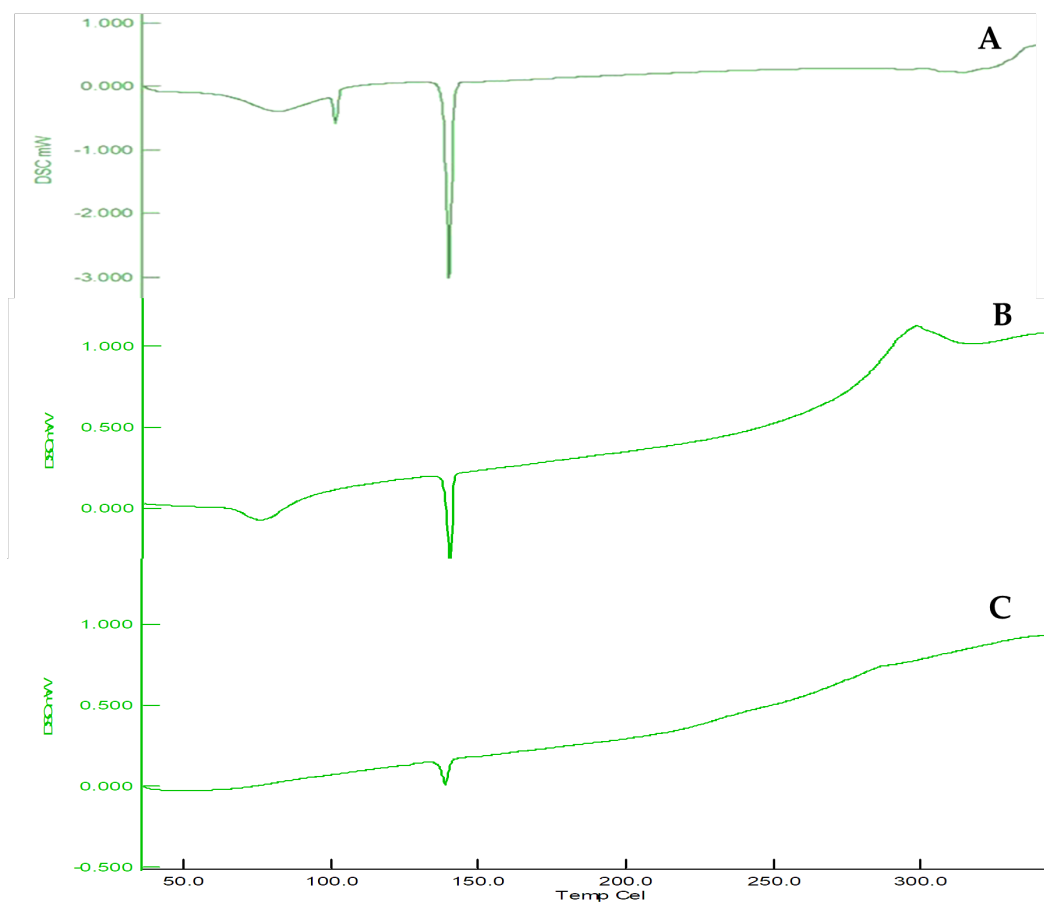


Figure 4: DSC of A) Pure drug, B) Physical mixture and C) lyophilized CH-NP.

of protonated amino group at 3198 cm^{-1} in physical mixture spectrum was shifted slightly to 3190.37 in CH-NP.

Differential Scanning Calorimetry

Figure 4 indicates differential scanning calorimetric graph for pure fluconazole, chitosan-fluconazole physical mixture, FZ CH-NP. In DSC curve of drug, narrow endotherm at 139.6°C was observed which represented the melting point for FZ. The curve of physical mixture retained the sharp endothermic peak of FZ at 139.6°C indicating its crystalline nature whereas in CH-NP, a low intensity broad endothermic peak for FZ was observed. This shows that during nanoparticle preparation, FZ transforms from a crystalline to an amorphous form.

X-ray Diffraction

The X-ray powder diffraction patterns, as depicted in Figure 5, provided additional confirmation of the aforementioned observations. The XRD pattern of fluconazole displayed distinct and intense peaks, indicating the crystalline nature of the drug. The physical mixture of chitosan and FZ showed the intense peaks of the FZ and the characteristics peak of chitosan. The XRD of chitosan nanoparticle revealed decrease in intensity of FZ characteristics peaks. This validates the drug's transition in NP from a crystalline to an amorphous state.

Formulation and optimization of gelatine-chitosan composite film

The polymer composite film was prepared using different concentration of gelatine and chitosan and also optimized for different concentration of plasticizer. Glycerine was used as plasticizer since it can improve flexibility and handling of films as well as maintain integrity by avoiding pores and cracks in the polymeric matrix.

Optimization of plasticizer concentration

The concentration of glycerine as plasticizer was optimized, at constant chitosan: gelatine ratio of 1:10, by checking peeling of formulated film from petri plate. These formulations were also evaluated for thickness, folding endurance and % water absorption (Table 4). It was found that all film formulations having 5 and 10% of glycerine can be easily peeled from petri plates maintaining its structure intact and there was not much effect on folding endurance of films with increasing plasticiser concentration. The thickness of film was found to be uniform between 0.45-0.51mm at all concentrations of glycerine. Since these films are designed for biological applications and has to be used in presence of biological fluid, capacity of film to absorb exudates is an important parameter to consider. Comparative evaluation of percent water absorption of film (Figure 6 a) was

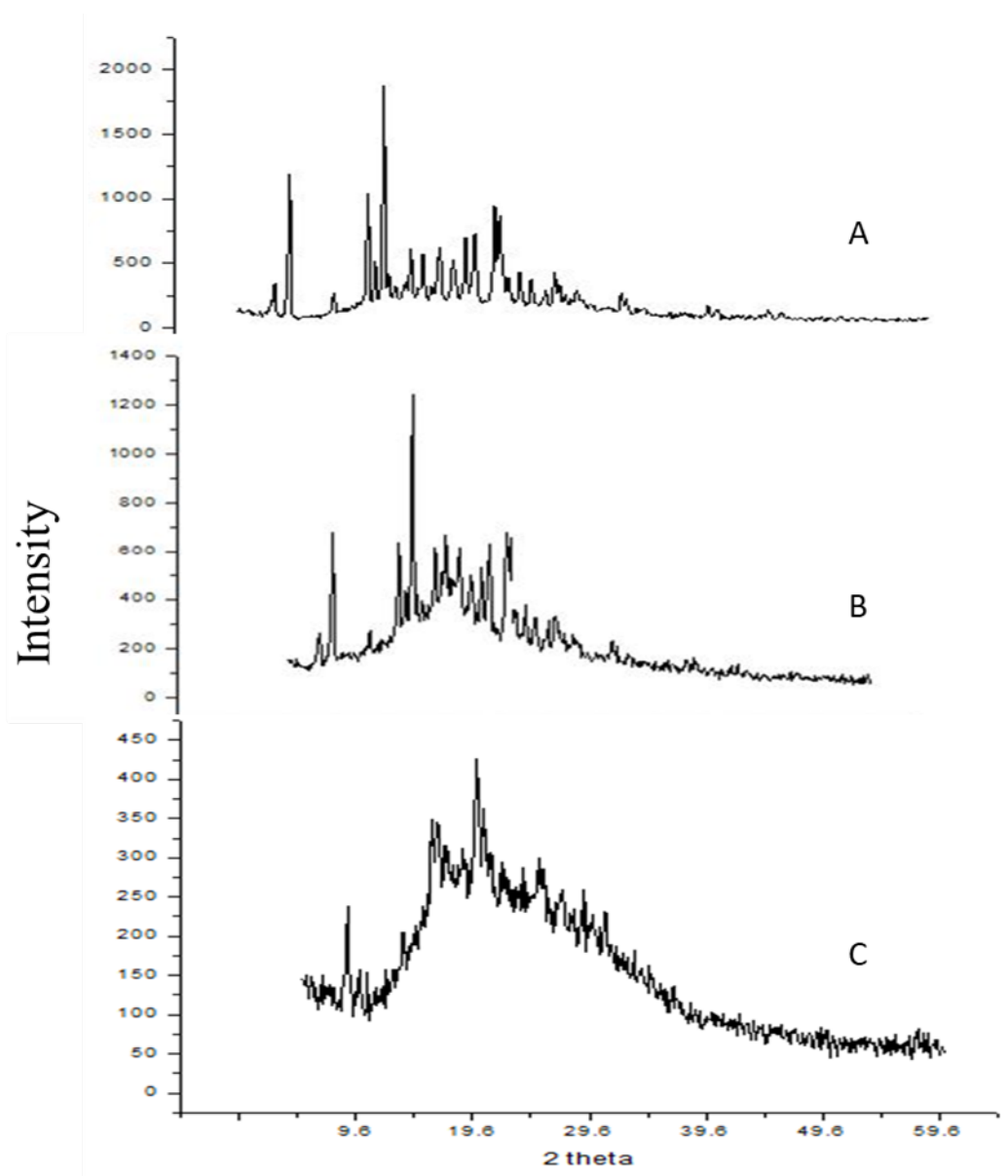


Figure 5: X-ray diffraction of A) Pure drug B) Physical mixture and C) Lyophilized CH-NP.

Table 4: Optimization of Plasticizer concentration.

Concentration of glycerine (%)	Peeling behaviour	Thickness	Folding Endurance	% water absorption			
				1 hr	2 hr	3 hr	24 hr
10	Easy	0.45	300	130.8	152.9	162.5	550.8
5	Easy	0.46	300	167.3	211.4	236.0	830.5
2.5	Difficult	0.46	300	195.8	257.9	354.8	976.1
1	Difficult	0.38	300	215.4	301.9	403.9	1205

found to be higher at lower concentration i.e. 1% of glycerine but peeling of film was found to be difficult; therefore, 5% of glycerine with comparatively higher water absorption and acceptable peeling behaviour was used as plasticizer for further studies.

Optimization of chitosan: gelatine concentration

The chitosan: gelatine ratio for preparation of film was optimized on the basis of its water absorption capacity. Comparative evaluation of % water absorption at 1:10, 1:20, 1:30 and 1:40

Table 5: Optimization of CH: gelatine ratio.

Chitosan: Gelatine Ratio	Thickness Mm	Folding endurance	% water absorption			
			1 hr	2 hr	3 hr	24 hr
1:10	0.45	300	356.6	528.2	620.0	1257.6
1:20	0.46	300	351.0	422.6	504.8	931.4
1:30	0.48	300	347.7	411.8	518.6	840.3
1:40	0.51	300	399.2	532.0	720.9	1163.4

chitosan: gelatine ratio is shown in (Table 5) and (Figure b). It was observed that low concentration of gelatine has higher absorption capacity as compared to higher concentration. All formulations have similar values of folding endurance as well as thickness. Lower and higher ratios of chitosan: gelatine was further selected for optimization of concentration of crosslinking agent.

Optimization of crosslinking agent

Formaldehyde was utilised for crosslinking of chitosan: gelatin film. Since, formaldehyde has greater access to lysine or to other reactive groups such as Cys and Hys present in gelatine molecule, it can result in an increase in the degree of crosslinking. The optimization of concentration of crosslinking agent was performed on the basis of percent water absorption (Figure c) and *in vitro* biodegradation behaviour (Figure 9). It was noted that a decrease in the quantity of crosslinking agent resulted in an increase in the percentage of water absorption. This phenomenon occurs because a lower amount of crosslinking agent reduces the molecular chain crosslinking density within chitosan-gelatin. Consequently, the chain network structure of the hydrogel molecule becomes loosely bound, creating more free space and leading to an enhanced water absorption capacity. Additionally, robust hydrophilic interactions between -OH, -COOH and -NH₂ groups contribute to the film's ability to retain a substantial amount of water, maintaining a higher degree of equilibrium swelling. Nevertheless, with an increase in the quantity of crosslinking agent, the crosslinking density of the film rises, resulting in a reduction of the network structure and grid. Consequently, the permeability of molecular water through the pore channels decreases leading to a decrease in the equilibrium swelling degree. However, a higher amount of crosslinking agent contributes to increased film rigidity, causing a loss of flexibility in its application. As per previous reports, 0.01% of formaldehyde is required for complete crosslinking of gelatine in formulation reducing the possibility of presence of free formaldehyde in formulation. Thus, this concentration was selected for *in vivo* studies.⁴¹

In vitro biodegradation

Comparative biodegradation results of formulation with low (1:10) and high ratio of chitosan: gelatine ratio with and without formaldehyde are shown in (Figure 7). Results indicated complete

biodegradation of uncross linked film within 2h, whereas increasing the concentration of crosslinking agent retarded the degradation rate of film from approximately 40 to 80 hr. There was no much change in biodegradation of films at 1:10 and 1:40 ratio of chitosan: gelatin in formulation, so ratio of 1:10 was used for further studies.

FZ CH-NP loaded films using 1:10 chitosan: gelatine ratio, 5% glycerine as plasticizer and 0.01, 0.02 and 0.03% of formaldehyde as crosslinking agent were evaluated for drug content and drug release and compared with films containing pure drug without NP (Figure 8). The content of the films was in the range of 94.11% to 96.33% of the theoretical concentration, with relative standard deviations ranged from 0.94% to 1.451% which indicated the content uniformity throughout the film. The drug release indicated sustained release behaviour from NP preparation compared to burst release from FZ films without NP. The drug release from FZ films without NP was 93.9±1.4% in 6 hr of dissolution whereas FZ release from CH-NP loaded films cross-linked with 0.01%, 0.02% and 0.03% formaldehyde was 93.2±1.2, 90.9±1.1 and 86.1±1.0% respectively. This data was fitted to various dissolution models to find out the mechanism of drug release. The highest values of correlation coefficient suggested Higuchi matrix as the best fit model (*n* value of K-P model as 0.5). Thus, the drug release in these formulations was governed by the drug diffusion through film matrix. From the above observations it was inferred that as fluconazole has moderate solubility, the drug release from composite film was not dependent on biodegradation of film and was completely controlled by diffusion across the film matrix.

Antifungal activity of composite film

The antifungal activity of FZ alone, FZ film and FZ CH-NP loaded film were carried out by time kill method using *Candida albicans* and results were compared with that of control without treatment. The control group after 2 and 6 hr showed dense growth as shown in Figure 9. Samples of FZ alone, FZ film and FZ CH-NP loaded film did not show any colonies after 2 hr as well as 6 hr indicating complete inhibition i.e. 6 log₁₀ reduction of *C. albicans*. This indicates antifungal efficacy of developed films and release of drug above its minimum inhibitory concentrations.

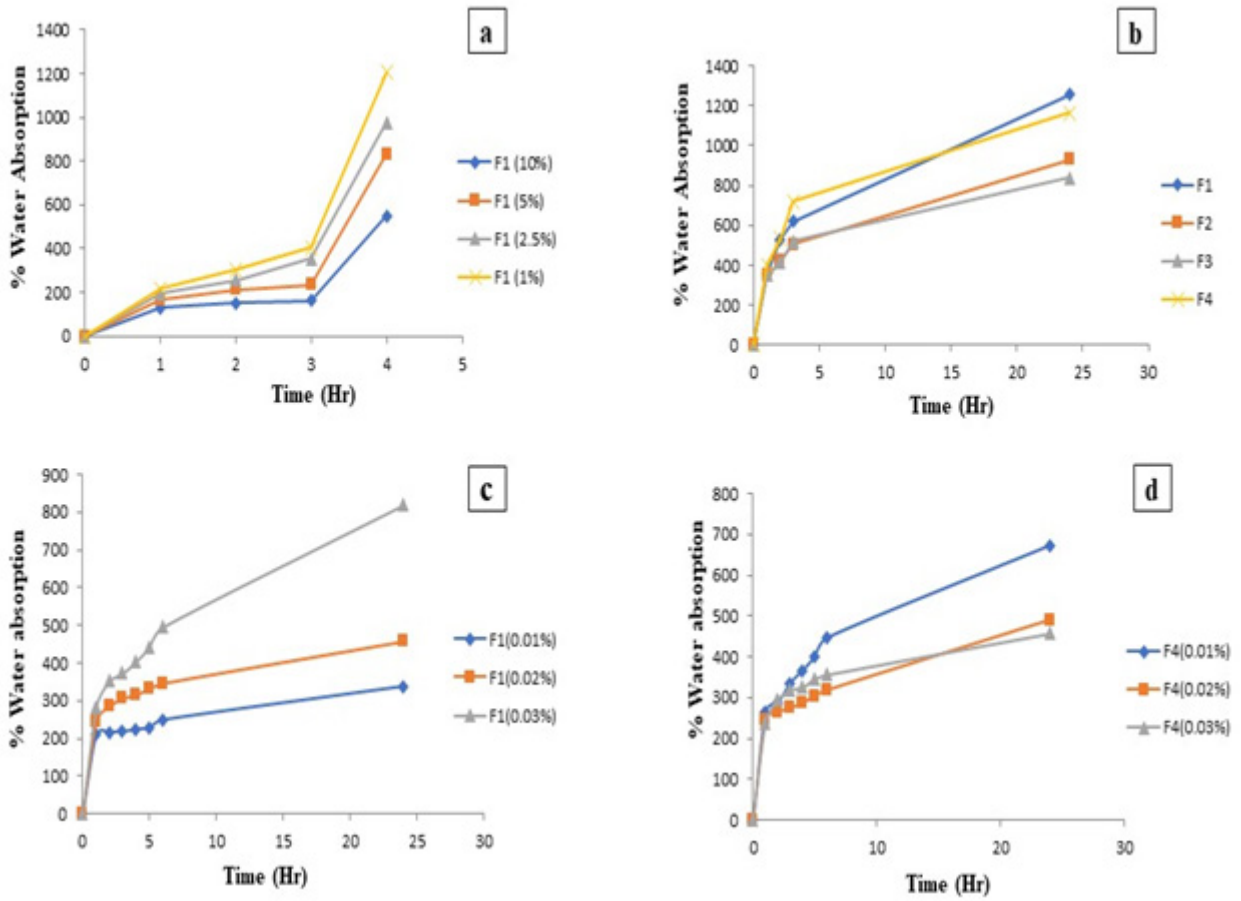


Figure 6: a. Effect of plasticizer concentration, b. Effect of chitosan: gelatine ratio, c and d: Effect of formaldehyde concentration.

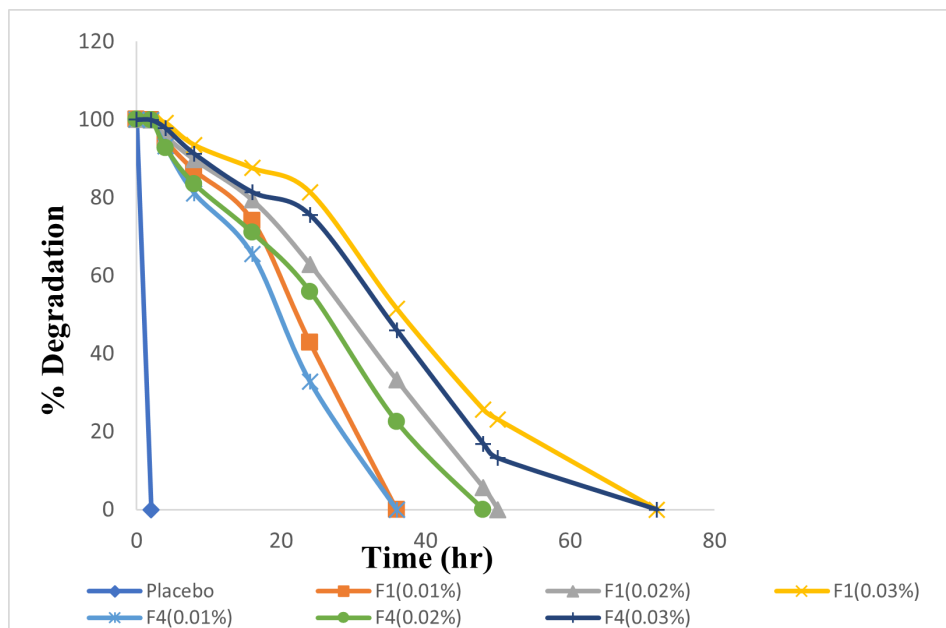


Figure 7: *In vitro* degradation of crosslinked formulations.

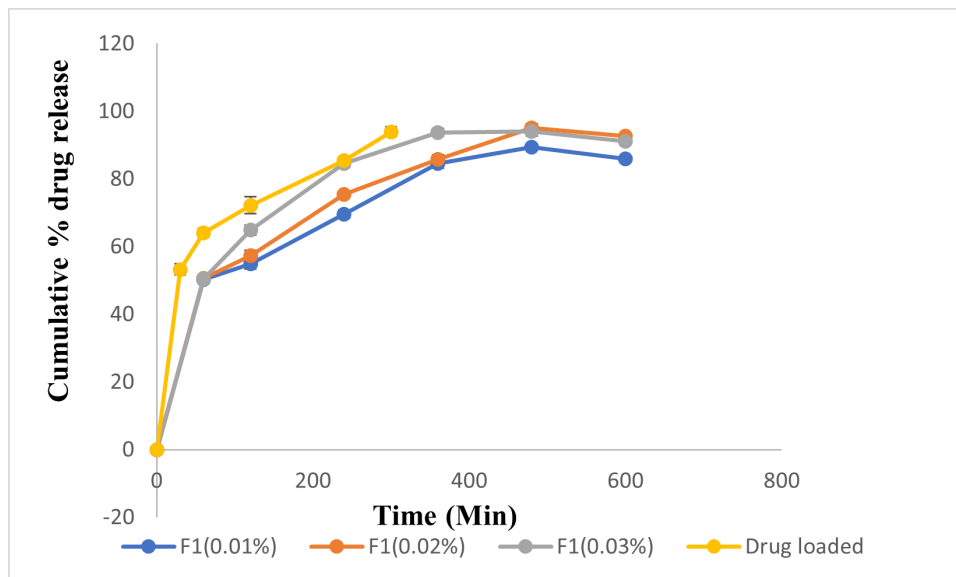


Figure 8: *In vitro* drug release of FZ CH-NP films and FZ films.



a

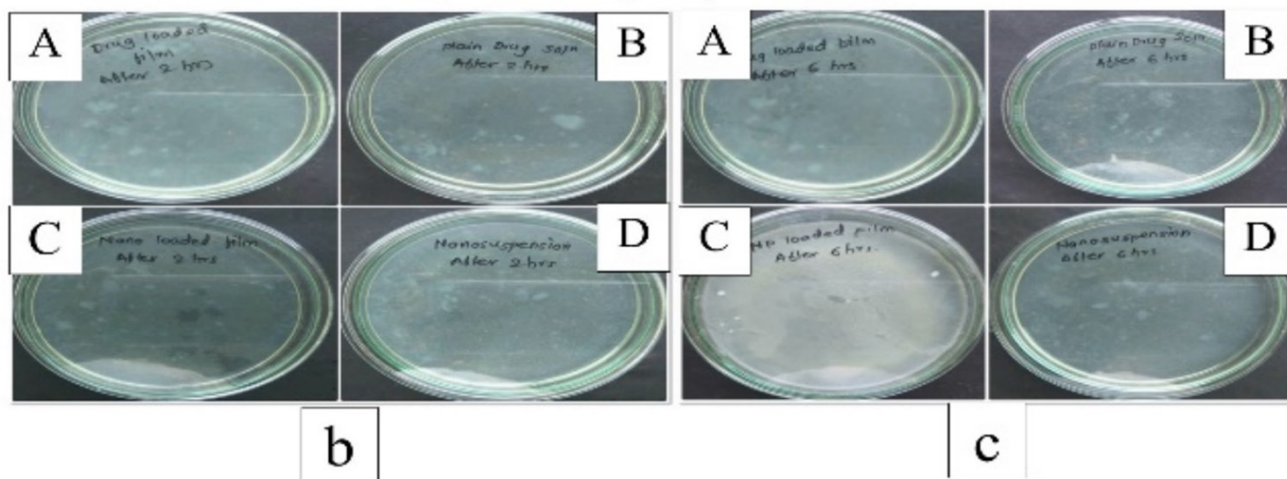


Figure 9: a. Control (Contact time: 2 hr), b: Observations after 2 hr A) Drug loaded film, B) FZ solution, C) FZ CH-NP film and D) FZ CH-NP, c: Observations after 6 hr A) Drug loaded film, B) FZ solution, C) FZ CH-NP film and D) FZ CH-NP.

In vivo biodegradation study

Preclinical studies were performed to check *in vivo* biodegradation of prepared implant and its acute toxicity studies in wistar rats. Formulations were implanted by making deep incisions at thigh region of rats and observed for biodegradation after opening operating site after 2, 5, 7, 14 and 21 days of implantation and

observing visually for presence of implant. The observations are indicated in Table 6 and Figure 10. It was observed that uncross linked implant showed complete biodegradation within 3-4 days whereas crosslinked implant [0.01% formaldehyde] showed the complete biodegradation within 7 days of implantation. This is in contrast to *in vitro* biodegradation study, where the degradation

Table 6: In vivo biodegradation of Implant.

Groups (n=5)	Degradation time				
	3 days	5 days	7 days	14 days	21 days
Group 1: (Control group)	No films were inserted				
Group 2: Film (Uncross Linked-Placebo)	Y	Y	Y	Y	Y
Group 3: Crosslinked-Plain Drug loaded film	N	N	Y	Y	Y
Group 4: Crosslinked-Nanoparticle loaded film	N	N	Y	Y	Y

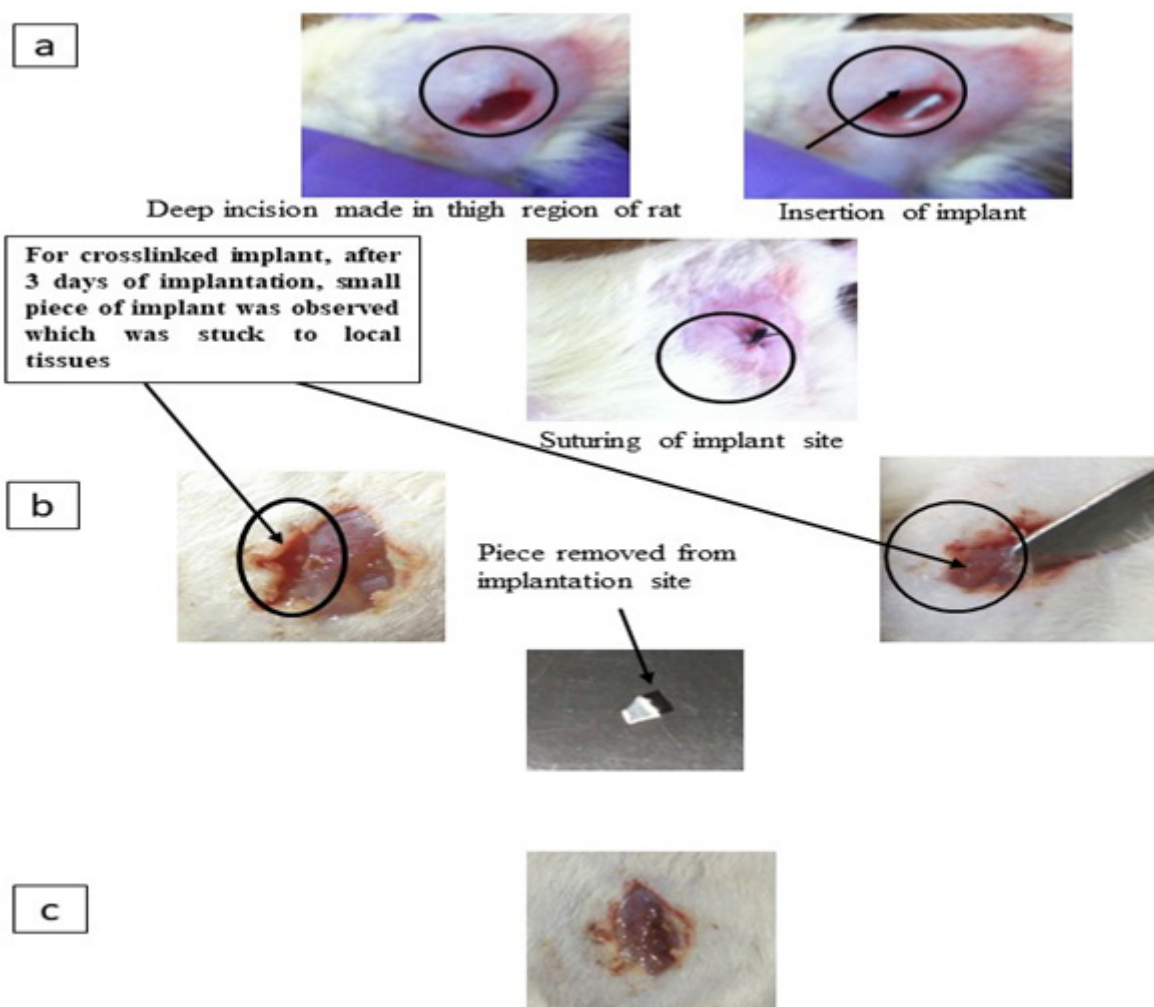


Figure 10: a. Procedure for implantation. b. Observations after implantation. c. Complete biodegradation of implant after 7 days.

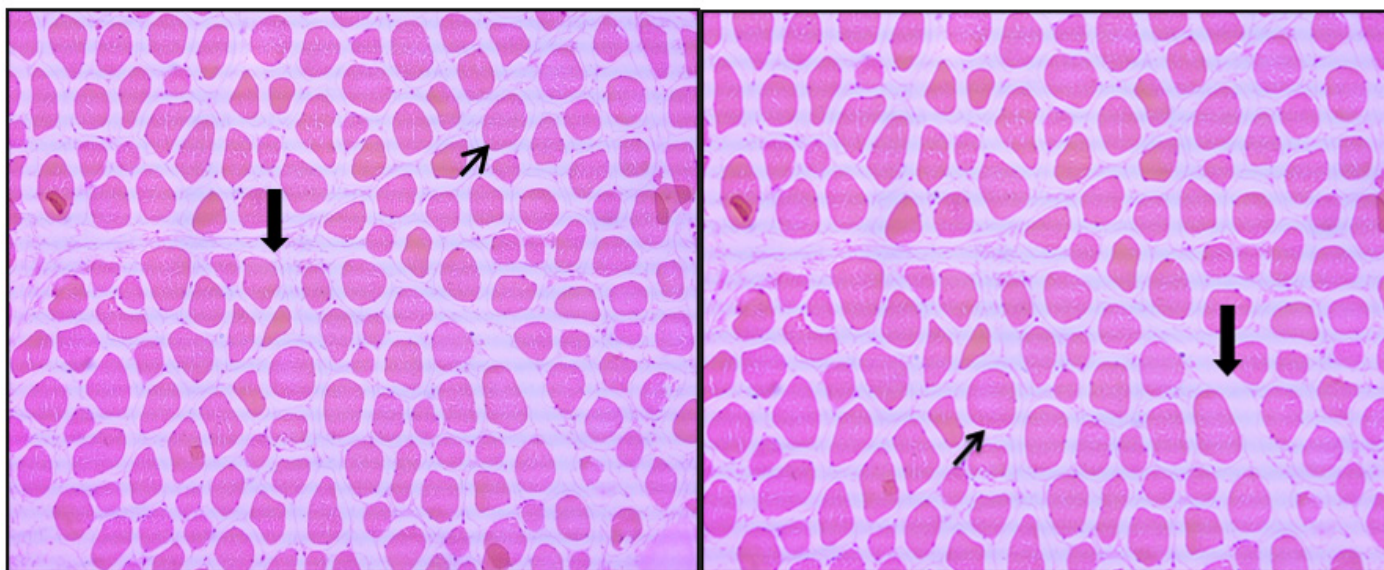


Figure-A

Figure-B

Figure 11: A and B: Histopathology of implant.

of crosslinked film was complete within the period of 1.5 to 3 days. This could be attributed to lower volume of fluid available *in vivo* in rodents for dissolution and degradation of film.

Microscopic examination of tissue of normal control group showed normal histology of musculature and the lesion revealed pathological significance (Figure 11). Histopathological examination of group treated with film also indicated normal muscle histology with no acute toxicity to muscle; hence the formulated nanoparticle loaded antifungal films were indicated as safe.

CONCLUSION

In this present study, we successfully developed fluconazole loaded chitosan nanoparticles with desirable entrapment efficiency, particle size and sustained drug release. FZ Nanoparticles were incorporated in gelatine and chitosan composite films and optimized for chitosan: gelatine ratio of 1:10, plasticizer concentration of 5% and crosslinker (formaldehyde) concentration as 0.01%. *In vitro* studied demonstrated sustained release of drug with potent *in vitro* antifungal activity and *in vitro* biodegradation within 3 days. The *in vivo* biodegradation studies of implant in rats showed complete degradation of film within 7 days of implantation. Histopathology studies revealed no acute toxicity of implanted formulation. Thus, Fluconazole based chitosan nanoparticle loaded composite films could serve as a potential approach to prevent fungal infections acquired during surgery.

ACKNOWLEDGEMENT

The authors would like to thank Dr. D.Y. Patil, Medical College, Hospital and Research Centre, Pune for providing culture of *Candida albicans*.

CONFLICT OF INTEREST

The authors declare that there is no conflict of interest.

ABBREVIATIONS

FZ: Fluconazole; **CH:** Chitosan; **NP:** Nanoparticles; **TPP:** Triphosphosphate; **Hr:** Hours; **FTIR:** Fourier Transform Infrared Spectroscopy; **DSC:** Differential scanning calorimetry; **XRD:** X-ray diffraction; **Fig:** Figure; **Min:** Minutes; **PMMP:** Polymethyl methacrylate.

REFERENCES

- Esteban J, Vallet-Regi M, Aguilera-Correa JJ. Antibiotics- and Heavy Metals-Based Titanium Alloy Surface Modifications for Local Prosthetic Joint Infections. *Antibiotics*. 2021;10(10):1270.
- Bhavani PRS, Desai DD, Manikkath J. Advances and Challenges In Development of Nanoparticulate Carriers for Ocular Applications: Focus on Ophthalmic Antifungal Drug Delivery Systems. *J Pharm Negat Results*. 2022;6834-50.
- Gupta H, Kumar S, Yadav D, Verma OP, Sharma TK, Ahn CW, et al. Data Analytics and Mathematical Modeling for Simulating the Dynamics of COVID-19 Epidemic—A Case Study of India. *Electronics*. 2021;10(2):127.
- Jiang P, Zhang Y, Hu R, Shi B, Zhang L, Huang Q, et al. Advanced surface engineering of titanium materials for biomedical applications: From static modification to dynamic responsive regulation. *Bioact Mater*. 2023;27:15-57.
- Antifungal activity of immunosuppressants used alone or in combination with fluconazole | *Journal of Applied Microbiology* | Oxford Academic [Internet]. [cited 2024 Jan 26]. Available from: <https://academic.oup.com/jambio/article-abstract/126/5/1304/6714972?login=false>
- Antifungal Activity of Capric Acid, Nystatin and Fluconazole and Their *in vitro* Interactions Against *Candida* Isolates from Neonatal Oral Thrush | *ASSAY and Drug Development Technologies* [Internet]. [cited 2024 Jan 26]. Available from: <https://www.liebertpub.com/doi/abs/10.1089/adt.2020.971>

7. Adlay Polyelectrolyte Multilayer Films Coated on Titanium: Surface Characteristics and MC3T3-E1 Cell Morphology and Proliferation | Boonbanyen | Journal of Health Science and Medical Research [Internet]. [cited 2024 Jan 26]. Available from: <https://www.jhsmr.org/index.php/jhsmr/article/view/987>
8. Chandra G, Pandey A. Biodegradable bone implants in orthopedic applications: a review. *Biocybern Biomed Eng.* 2020;40(2):596-610.
9. Enhancing the Antifungal Activity and Ophthalmic Transport of Fluconazole from PEGylated Polycaprolactone Loaded Nanoparticles-PMC [Internet]. [cited 2024 Jan 26]. Available from: <https://www.ncbi.nlm.nih.gov/pmc/articles/PMC9823753/>
10. Zainab S, Hamid S, Sahar S, Ali N. Fluconazole and biogenic silver nanoparticles-based nano-fungicidal system for highly efficient elimination of multi-drug resistant Candida biofilms. *Mater Chem Phys.* 2022;276:125451.
11. Riaz T, Tande AJ, Steed LL, Demos HA, Salgado CD, Osmon DR, et al. Risk Factors for Fungal Prosthetic Joint Infection. *J Bone Jt Infect.* 2020;5(2):76-81.
12. Feng Y, Chang L, Zhu S, Yang Y, Wei B, Lv M, et al. Preparing a Bioactive (Chitosan/Sodium Hyaluronate)/SrHA Coating on Mg-Zn-Ca Alloy for Orthopedic Implant Applications. *Front Mater [Internet].* 2022 [cited 2024 Jan 26];8. Available from: <https://www.frontiersin.org/articles/10.3389/fmats.2021.823506>
13. Tiwari A, Yadav AK, Bagaria V. Chapter 17-Nanomaterials-based antimicrobial coatings for medical devices. In: ul Islam S, Hussain CM, Shukla SK, editors. *Antiviral and Antimicrobial Coatings Based on Functionalized Nanomaterials [Internet]. Elsevier;* 2023 [cited 2024 Jan 26]. p. 545-68. Available from: <https://www.sciencedirect.com/science/article/pii/B9780323917834000085>
14. Enzymatic co-crosslinking of star-shaped poly(ethylene glycol) tyramine and hyaluronic acid tyramine conjugates provides elastic biocompatible and biodegradable hydrogels-PMC [Internet]. [cited 2024 Jan 26]. Available from: <https://www.ncbi.nlm.nih.gov/pmc/articles/PMC9127275/>
15. El Sayeh F, Abou El Ela A, Abbas Ibrahim M, Alqahtani Y, Almomen A, Sfouq Aleanizy F. Fluconazole nanoparticles prepared by antisolvent precipitation technique: Physicochemical, *in vitro*, *ex vivo* and *in vivo* ocular evaluation. *Saudi Pharm J.* 2021;29(6):576-85.
16. Hassan DM, El-Kamel AH, Allam EA, Bakr BA, Ashour AA. Chitosan-coated nanostructured lipid carriers for effective brain delivery of Tanshinone IIA in Parkinson's disease: interplay between nuclear factor-kappa β and cathepsin B. *Drug Deliv Transl Res.* 2024;14(2):400-17.
17. SURIYAAMPORN P, สุริยาอำพร, NGAWHIRUNPAT T, ฐาริษฐิพัฒน์, University S, NGAWHIRUNPAT T, et al. Development of two-layer dissolving microneedles loading fluconazole microemulsions for ocular drug delivery [Internet] [Thesis]. Silpakorn University; 2023 [cited 2024 Jan 26]. Available from: <http://thesis-ir.su.ac.th:8080/jspui/handle/123456789/4472>
18. Higino T, França R. Drug-delivery nanoparticles for bone-tissue and dental applications. *Biomed Phys Eng Express.* 2022;8(4):042001.
19. Almehmady AM, El-Say KM, Mubarak MA, Alghamdi HA, Somali NA, Sirwi A, et al. Enhancing the Antifungal Activity and Ophthalmic Transport of Fluconazole from PEGylated Polycaprolactone Loaded Nanoparticles. *Polymers.* 2023;15(1):209.
20. Frontiers | Progress of polymer-based strategies in fungal disease management: Designed for different roles [Internet]. [cited 2024 Jan 26]. Available from: <https://www.frontiersin.org/articles/10.3389/fcimb.2023.1142029/full>
21. IJMS | Free Full-Text | New Approach to Antifungal Activity of Fluconazole Incorporated into the Porous 6-Anhydro- α -l-Galacto- β -d-Galactan Structures Modified with Nanohydroxyapatite for Chronic-Wound Treatments-*in vitro* Evaluation [Internet]. [cited 2024 Jan 26]. Available from: <https://www.mdpi.com/1422-0067/22/6/3112>
22. Araujo HC, Pessan JP, Caldeirão ACM, Sampaio C, Oliveira MJ dos S, Sales DH, et al. Dual nanocarrier of chlorhexidine and fluconazole: Physicochemical characterization and effects on microcosm biofilms and oral keratinocytes. *J Dent.* 2023;138:104699.
23. Costa-Pinto AR, Lemos AL, Tavará FK, Pintado M. Chitosan and Hydroxyapatite Based Biomaterials to Circumvent Periprosthetic Joint Infections. *Materials.* 2021;14(4):804.
24. Yadav TC, Gupta P, Saini S, Mohiyuddin S, Pruthi V, Prasad R. Plausible Mechanistic Insights in Biofilm Eradication Potential against *Candida* spp. Using *in situ*-Synthesized Tyrosol-Functionalized Chitosan Gold Nanoparticles as a Versatile Antifouling Coating on Implant Surfaces. *ACS Omega.* 2022;7(10):8350-63.
25. Amreen S, Shahidulla D, Sultana A, Fatima N. Implantable Drug Delivery System: An Innovative Approach. *J Drug Deliv Ther.* 2023;13:98-105.
26. JBJI-Prosthetic-joint Infections: Mortality Over the Last 10 Years [Internet]. [cited 2024 Jan 26]. Available from: <https://jbj.copernicus.org/articles/4/198/2019/>
27. Manufacturing Considerations for Implantable Drug-Delivery Systems-Medical Design Briefs [Internet]. [cited 2024 Jan 26]. Available from: <https://www.medicaldesignbriefs.com/component/content/article/48785-manufacturing-considerations-for-implantable-drug-delivery-systems>
28. Bashir K, Chen G, Han J, Shu H, Cui X, Wang L, et al. Preparation of magnetic metal organic framework and development of solid phase extraction method for simultaneous determination of fluconazole and voriconazole in rat plasma samples by HPLC. *J Chromatogr B.* 2020;1152:122201.
29. Pluronic F-127 Enhances the Antifungal Activity of Fluconazole against Resistant *Candida* Strains | ACS Infectious Diseases [Internet]. [cited 2024 Jan 26]. Available from: <https://pubs.acs.org/doi/full/10.1021/acscinfecdis.3c00536>
30. A. Aygün, Synthesis and characterization of Reishi mushroom-mediated green synthesis of silver nanoparticles for the biochemical applications *J. Pharmaceut. Biomed. Anal.* (2020)
31. Brambilla, E.; Locarno, S.; Gallo, S.; Orsini, F.; Pini, C.; Farronato, M.; et al. Poloxamer-Based Hydrogel as Drug Delivery System: How Polymeric Excipients Influence the Chemical-Physical Properties. *Polymers* 2022, 14, 3624.
32. Kurniawansyah, I.S.; Rusdiana, T.; Sopyan, I.; Ramoko, H.; Wahab, H.A.; Subarnas, A. *In situ* ophthalmic gel forming systems of poloxamer 407 and hydroxypropyl methyl cellulose mixtures for sustained ocular delivery of chloramphenicol: Optimization study by factorial design. *Heliyon* 2020, 6, e05365.
33. Liu, Y.; Cui, X.; Zhao, L.; Zhang, W.; Zhu, S.; Ma, J. Chitosan Nanoparticles to Enhance the Inhibitory Effect of Natamycin on *Candida albicans*. *J. Nanomater.* 2021, 2021, 6644567.
34. Winkler, J.S.; Barai, M.; Tomassone, M.S. Dual drug-loaded biodegradable Janus particles for simultaneous co-delivery of hydrophobic and hydrophilic compounds. *Exp. Biol. Med.* 2019, 244, 1162-77.
35. Sharma DS, Wadhwa S, Gulati M, Kumar B, Chitranshi N, Gupta VK, et al. Chitosan modified 5-fluorouracil nanostructured lipid carriers for treatment of diabetic retinopathy in rats: a new dimension to an anticancer drug. *Int J Biol Macromol.* 2023;224:810-30.
36. Eid RK, Ashour DS, Essa EA, El Maghraby GM, Arafa MF. Chitosan coated nanostructured lipid carriers for enhanced *in vivo* efficacy of albendazole against *Trichinella spiralis*. *Carb Polym.* 2020;232:115826.
37. Nehal N, Nabi B, Rehman S, Pathak A, Iqbal A, Khan SA, et al. Chitosan coated synergistically engineered nanoemulsion of Ropinirole and nigella oil in the management of Parkinson's disease: formulation perspective and *in vitro* and *in vivo* assessment. *Int J Biol Macromol.* 2021;167:605-19.
38. Sherawat K, Mehan S. Tanshinone-IIA mediated neuroprotection by modulating neuronal pathways. *Naunyn Schmiedebergs Arch Pharmacol.* 2023;396:1647-67.
39. Witika BA, Poka MS, Demana PH, Matafwali SK, Melamane S, Malungelo Khamanga SM, et al. Lipid-based nanocarriers for neurological disorders: a review of the state-of-the-art and therapeutic success to date. *Pharmaceutics.* 2022;14.
40. Abhangi KV, Patel JI. Neuroprotective effects of linagliptin in a rotenone-induced rat model of Parkinson's disease. *Indian J Pharmacol.* 2022;54:46-50.
41. Kale RN, Bajaj AN, Ultraviolet Spectrophotometric Method for Determination of Gelatin Crosslinking in the Presence of Amino Groups: *J Young Pharm.* 2010;2(1):90-4.

Cite this article: Kale R, Deshkar SS, Deshmane PD, Whagmare B. Development of Nanoparticle-Based Biodegradable Polymer Composite Film for Antifungal Drug Delivery in Prosthetic Joint Infection. *Indian J of Pharmaceutical Education and Research.* 2024;58(2s):s468-s483.